Volume 4, Issue 1, 2015, 236-240 ISSN 2284-6808

Letters in Applied NanoBioScience

www.NanoBioLetters.com

Original Research Article Open Access Journal

Received: 20.10.2014 / Revised: 25.12.2014 / Accepted: 15.02.2015 / Published on-line: 30.03.2015

Effects of DMSA-Fe_2O_3@DOX nanoconjugate on tumor HEPG2 cells

Guowei Hu [1,†], Song Zhang [1,†], Lulu Zhang [1], Fuming He [1], Xin Wang [1], Xinli Liu [1,*]

[1]Shandong Provincial Key Laboratory of Microbial Engineering, Qilu University of Technology, Jinan, Shandong Province, P.R. 250353, China

[†]*The authors contributed equally to this study and share first authorship*

*corresponding author e-mail address:***vip.lxl@163.com***

ABSTRACT

Magnetic nanoparticles that bind with drugs are regarded as innovative, convenient, and highly efficient systems of drug delivery. In this study, the magnetic nanoparticle Fe_2O_3 was synthesized using the chemical co-precipitation method and modified with meso-2,3-dimercaptosuccinic acid (DMSA) to prevent the aggregation of nanoparticles. Doxorubicin hydrochloride (DOX) was immobilized on the surface of DMSA-Fe_2O_3 nanoparticles by electrostatic attraction. DMSA-Fe_2O_3 and DMSA-Fe_2O_3 loading DOX (DMSA-Fe_2O_3@DOX) were characterized by transmission electron microscopy, vibrating sample magnetometer, ultraviolet and visible spectrophotometer, and Fourier transform infrared spectroscopy, respectively. The results indicated that DOX can be successfully loaded on the surface of nanoparticles. The optimal condition was observed at a DOX concentration of 17μg/mL, adsorption time of 12 h and pH of 8.9 in magnetic nanoparticles suspension (1mg/mL), achieving a DOX loading rate as high as 87%. DMSA-Fe_2O_3 did not exhibit significant cytotoxic activity with regard to HepG2 cells; activity was slightly higher in DMSA-Fe_2O_3@DOX-treated cells compared to cells that were treated with DOX alone.

Keywords: *Iron oxide, magnetic materials, doxorubicin hydrochloride, nanoparticles, drug targeting.*

1. INTRODUCTION

Today, cancer is one of the most dangerous threats to human health, worldwide. It was estimated that 11,660,290 new cancer cases and 580,350 cancer deaths would occur in the United States alone in 2013 [1]. Doxorubicin hydrochloride (DOX) is one of the most efficacious drugs in the treatment of a broad range of cancers, including those of the breast, lung, and stomach, as well as sarcoma. Nevertheless, cardiotoxicity [2] and acquired resistance [3] limit its clinical application. A satisfactory solution is to design targeted drugs that not only deliver the drug to the tumor sites, but also protect normal cells from the unwanted toxic side effects [4]. In this respect, Fe_2O_3 nanoparticles have been widely used in drug delivery, because of their high level of biocompatibility and specificity [5-9].In the present study, we investigated a simple and effective approach for targeting DOX. The Fe_2O_3 nanoparticles were synthesized and modified by anionic compound meso-2,3-dimercaptosuccinic acid DMSA, which was modified on the surface of nanoparticles to prevent their aggregation. Furthermore, complex DMSA-Fe_2O_3 possesses a hydrophilic surface and functional groups, such as carboxylic groups, which may be further connected with DOX molecules to form a targeted drug.

2. EXPERIMENTAL SECTION

2.1. Synthesis.

Fe_2O_3 nanoparticles were synthesized according to the method reported [10-12]. Approximately 5.16 g of $FeCl_3 \cdot 6H_2O$ and 3.54 g of $FeSO_4 \cdot 4H_2O$ were dissolved in 100 mL deionized water in a three-necked flask under mechanical stirring. Subsequently, 12 mL ammonia solution (25%, w%) was rapidly added to the above solution. The solution immediately became black and the mixture was allowed to react for 40 min under the condition of N_2 flow. The formed Fe_3O_4 nanoparticles were washed immediately with distilled water five times by magnetic separation, and distributed in 400 mL deionized water with pH 3.0. The Fe_3O_4 nanoparticles were then oxided into a more stable formation (Fe_2O_3) by air pump under mechanical stirring for 2 h at 90°C. The Fe_2O_3 nanoparticle suspensions were consequently dispersed in 800 mL deionized water with a pH of 2.7, regulated by hydrochloric acid. Added to a solution of DMSA (0.2596 g) that was dissolved in slight amounts of acetone, the magnetic nanoparticle suspension was mechanically stirred for 4 h at room temperature. A generated coffee-colored product was then separated from the solution by a magnet. The particles were sequentially washed three or four times with deionized water.

According to electrostatic attraction, DOX was immobilized on the surface of DMSA-Fe_2O_3 nanoparticles [13]. In brief, DOX was firstly dissolved in deionized water (20 mL), and various amounts were added to the DMSA-Fe_2O_3 nanoparticle suspension and incubated at room temperature for 12 h to explore conjugation efficiency. The DMSA-Fe_2O_3 nanoparticle solution was then incubated in the same concentration of DOX for different times and at different pH values. The mixture was centrifuged and the DOX concentration in the supernatant was measured using ultraviolet and visible spectrophotometer (UV) at a wave length of 234.0 nm. The mass of conjugated DOX can be calculated by comparison with the standard DOX concentration curve.

2.2. Cell culture.

HepG2 cells (a human hepatoma cell line) were acquired from the Chinese Academy of Sciences and cultivated at 37°C in a

humidified 5% CO_2 incubator in RPMI-1640 supplemented with 10% fetal bovine serum, 100 units/ml penicillin, and 100 µg/ml streptomycin. The cells were in the long phase prior to the following experiments.

2.3. Cytotoxicity and morphology assessment.

HepG2 cell cytotoxicity of the DMSA-Fe_2O_3 nanoparticle, DOX, and the DMSA-Fe_2O_3@DOX nanoparticle was assessed using MTT assay. The cells were seeded in 12-well plates and treated with specific concentrations of these three materials. Untreated cells were used as a control group, and cell viability was examined after 24 h, 36 h, and 72 h of incubation. A total of 100 µl of MTT solution (5 mg/mL) was added to each well, which contained 1 ml of media, and these were incubated for 4 h at 37 °C in a humidified 5% CO_2 atmosphere. The media with MTT solution was subsequently removed and crystals of formazan from each well were suspended in 1 ml of dimethylsulfoxide. The plate was left on a shaking platform for 5 min, and the absorbance was recorded on a Microplate Reader at the length of 570 nm. The cell viability fraction (%) was calculated as:

Cell viability fraction (%) = mean experimental absorbance/mean control absorbance×100. Each assay was repeated at least three times.

Changes in cells morphology were determined by light microscope TELAVAL 3 and transmission electron microscope JEOL-1200EX. The cells were cultured with IC_{50} concentrations of DMSA-Fe_2O_3 nanoparticle, DOX, and DMSA-Fe_2O_3@DOX nanoparticle for 24, 48, and 72 h. They were then chipped into tissue blocks of 1.0 mm^3 on ice, immediately put into 3% glutaraldehyde in cacodilate buffer at 4°C for 2 h, and subsequently post fixed in a 1% osmium-tetroxide phosphate buffer solution for 1 h. The samples were then dehydrated in a graded ethanol series with acetone, and permeated and embedded in epoxide resin. Semithin sections of approximately 75 nm were prepared and stained with uranyl acetate and lead citrate, and were examined under an JEOL-1200EX transmission electron microscope.

3. RESULTS SECTION

Fe_2O_3 magnetic nanoparticles were synthesized using co-precipitation under a controlled condition. The synthesis of Fe_2O_3 magnetic nanoparticles, the modification of DMSA, and the loading of DOX, respectively, are shown in Fig. 1 [14, 15].

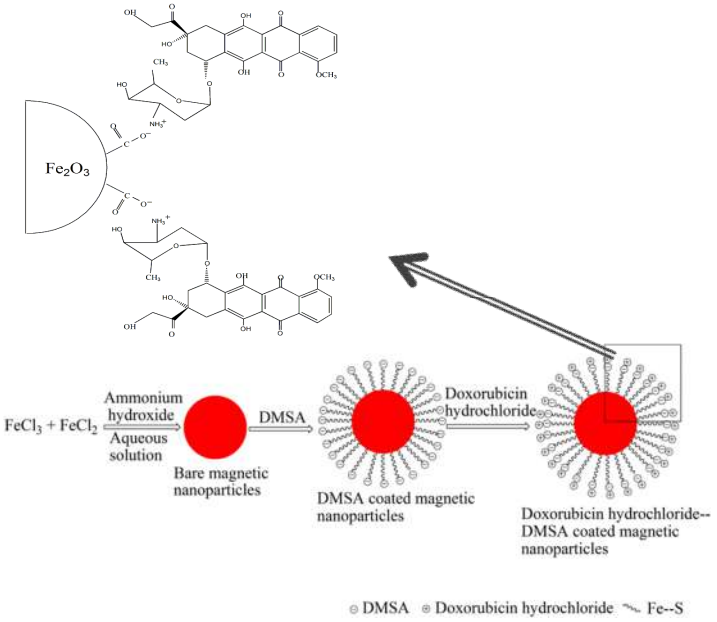

Figure 1. The process and mechanism of Fe_2O_3 magnetic nanoparticle synthesis, modification of DMSA and the loading of DOX.

The aggregation of un-modified Fe_2O_3 nanoparticles can generally be easily formed. To improve colloidal stability during the process of Fe_2O_3 nanoparticle and DOX interaction, the nanoparticles were coated with DMSA, which can link to their surface via the linkage of chemicals such as Fe-S [16]. Addition of DMSA to the surface of nanoparticles can improve dispersion in water because the addition of $–COO^-$ functions on the surface of nanoparticles affords a repulsive barrier. Moreover, positive drugs can be attached by negative ionic bonds, such as DOX [17].

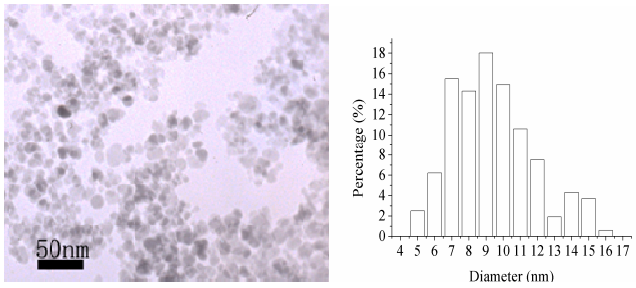

Figure 2. TEM micrographs for DMSA-Fe_2O_3 nanoparticles and particle size distribution.

The micrographs of the DMSA-Fe_2O_3 nanoparticles and the size distributions are shown in Figure 2, which confirms the formation of Fe_2O_3 nanoparticles as being spherical in shape, and their average size is approximately 10 nm. They can disperse stably in distilled water.

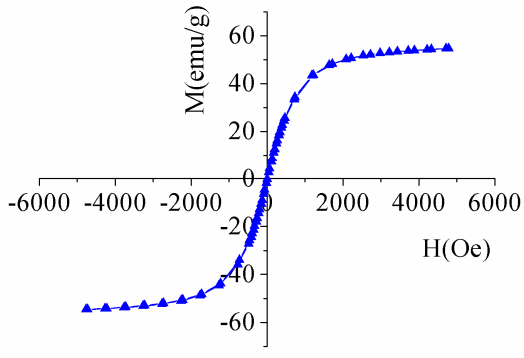

Figure 3. Room temperature magnetic hysteresis loop of DMSA-Fe_2O_3 nanoparticles.

As shown in Figure 3, saturation is observed around 3000 Oe, with a magnetic moment of 52.68 emu/g. Since the magnetic properties of materials are influenced by small size [18], the coercivity of DMSA-Fe_2O_3nanoparticles is close to zero, so they show a superparamagnetic property.

Figure 4 shows the Fourier transform infrared spectroscopy spectra of DMSA-Fe_2O_3 nanoparticles, DOX, and DMSA-Fe_2O_3@DOX. In spectrum a, the major characteristics of DOX peaks for the N-H bending, C=O absorbance band, and N-H stretching are observed at 1616, 1730, and 3327 cm^{-1}, respectively. In spectrum b, the presence of weak methylene peaks at 2924 and 2852 cm^{-1}, indicating that DMSA remained on the surface of Fe_2O_3 nanoparticles after modification. The sharp peaks at 634 and 586 cm^{-1} are Fe-O lattice vibration (stretching and bending vibration) [14]. In spectrum c, the major characteristics suggested that the strong and wide peak at 3394 cm^{-1} was related to the OH group vibrations, which had an overlap with NH_2 group vibrations. The presence of primary N-H groups in the drug molecular structure was detected in the IR spectrum at 1614 cm^{-1}, truly confirming the existence of the DOX on the nanoparticles. Characteristic DOX N-H group peak shifted from 1616 to1614 cm^{-1} ($^{\Delta}v$=2 cm^{-1})[20]. It can also bededuced that the DOX is efficiently loaded on the NPs. Other peaks in spectra showed a good consistency with the peaks, as evidenced by the pure DOX and Fe_2O_3-DMSA spectra in Figure 4.

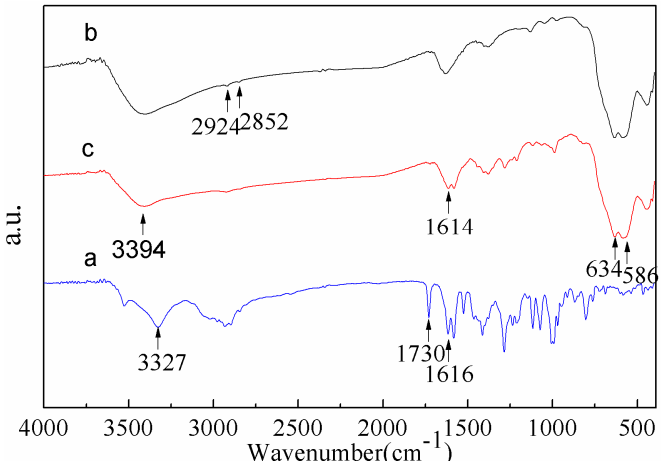

Figure 4. FTIR spectra: a) DOX; b) DMSA-Fe_2O_3 nanoparticle; c) DOX loaded on DMSA-Fe_2O_3 nanoparticle.

The loading capacity of DOX on DMSA-Fe_2O_3 nanoparticles was determined by UV spectrum at 234 nm, which is calculated by the difference in DOX concentrations between the original DOX solution and the supernatant solution after loading. Adsorption ratio (AR) of drug is defined using the following equation:

AR(%)=[mass of DOX initially added-mass of DOX in supernatant]/mass of DOX initially added ×100 (%)

As shown in Figure 5c, the adsorption ratio of DOX increased with increasing DOX concentration, which is attributed to the effect of complexation of drug with surfactant. The effect of various times (2-22h) on the AR can be evaluated by DMSA-Fe_2O_3 hydrogel. The optimal loading time was approximately 12h (Fig.5a). The maximum AR of the hydrogel was observed at a pH of 8.9 (Fig.5b), which was attributed to complete deprotonationof the carboxyl groups of DMSA-Fe_2O_3. During alkalinization, the DMSA-Fe_2O_3 released more –COO, which can be linked with DOX.

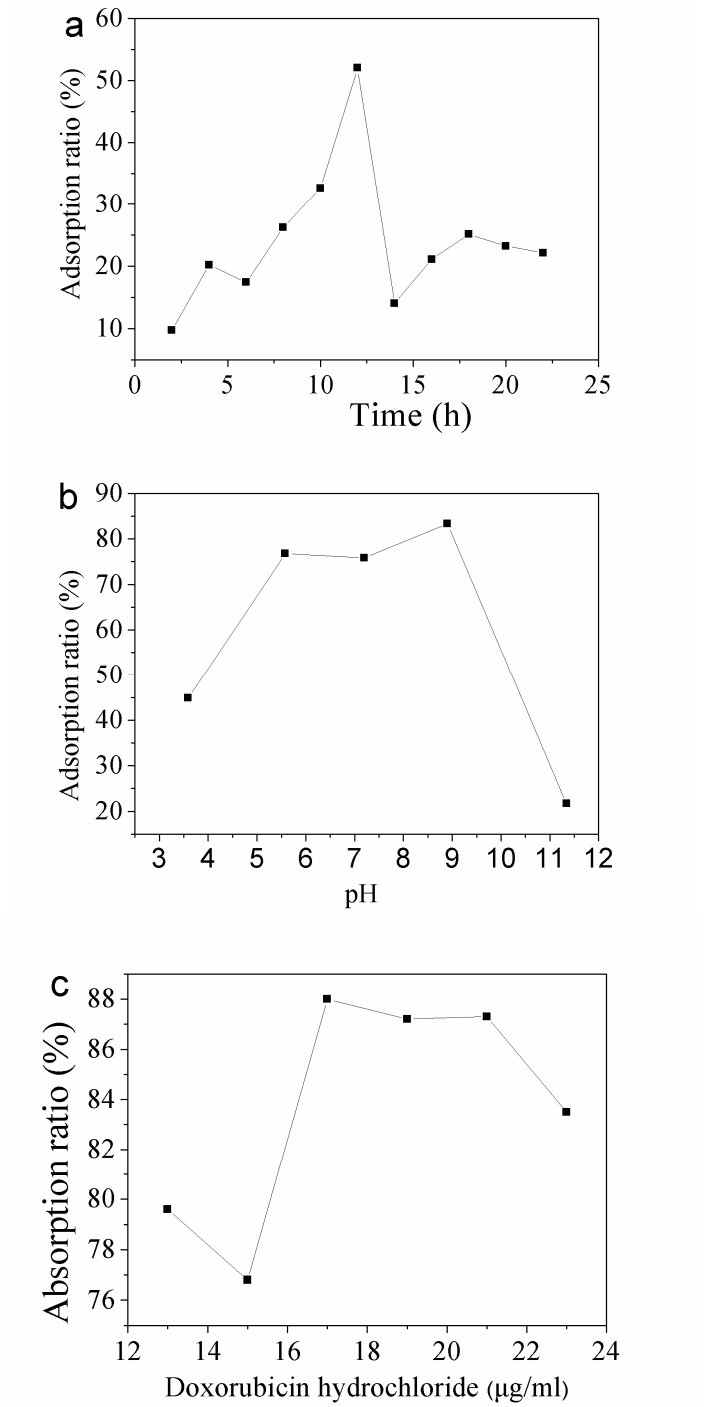

Figure 5. The effect of various factors on the adsorption ratio of DOX by DMSA-Fe_2O_3. a) loading time; b) loading pH; c) loading concentration of DOX.

The HepG2 cell cytotoxicity of DMSA-Fe_2O_3 nanoparticles, DMSA-Fe_2O_3@DOX nanoparticles, and DOX was evaluated by MTT assay after 24, 48, and 72 h of incubation. Our data showed that magnetic nanoparticles did not exhibit significant cytotoxic activity in HepG2 cells (Fig. 6). When treated with DMSA-Fe_2O_3 magnetic nanoparticles, approximately 90% of the cells survived (Fig. 6), which is consistent with the results of previous studies. In turn, DOX and DMSA-Fe_2O_3@DOX nanoparticle treatment resulted in great increasing HepG2cell inhibition (Fig. 6). Compared with DOX, the viability of HepG2 cells treated with DMSA-Fe_2O_3@DOX was lower. Moreover, lethality increased with increasing time, indicating a time-dependent effect *in vitro*. The increased cytotoxicity was likely due to improved DOX cellular uptake by the DMSA-Fe_2O_3@DOX

drug delivery system.In addition, the optical microscopic and TEM observations confirmed the MTT results, as shown in Figure 7. The untreated HepG2 cells attached to the plate in a normal shape. However, the cells treated with DOX and DMSA-Fe_2O_3@DOX showed sharp morphological changes (Fig. 7A). These cells were shrunken, and we observed a massive detachment from the culture plates, which indicated that these cells may have undergone cell death.At the same time, the mitochondria membrane and nucleolus vanished in the DMSA-Fe_2O_3@DOX group (Fig. 7B), demonstrating their synergistic anticancer activity. Typical apoptotic morphology became more apparent in cells treated with DMSA-Fe_2O_3@DOX, than that in cells treated with DOX alone, while convoluted nuclei with cavitations, fragmentation of the nucleus, and apoptotic bodies were observed after treatment with both DOX and DMSA-Fe_2O_3@DMSA. There was almost no evidence of apoptosis in the control group and DMSA-Fe_2O_3 group, which reliably supports the hypothesis that DMSA-Fe_2O_3@DOX could enhance DOX-induced cell apoptosis.Cell viability decreases with increasing concentrations of equivalent doses of DOX or nanoparticle and this is expressed as a percentage of the control value.

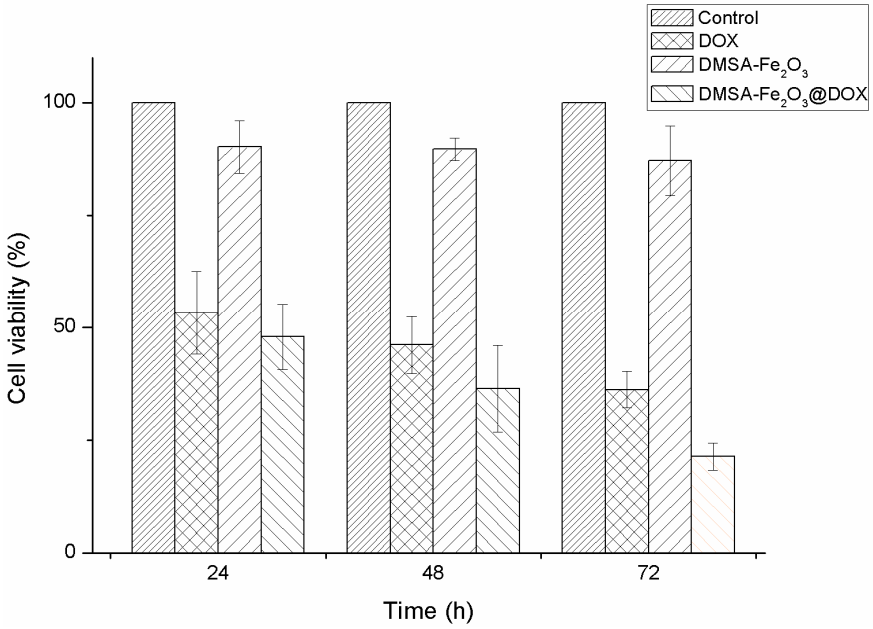

Figure 6. Cytotoxicity of DMSA-Fe_2O_3 magnetic nanoparticles, DOX and DMSA-Fe_2O_3@DOX on HepG2 cells after 24, 48, and 72 h of incubation.

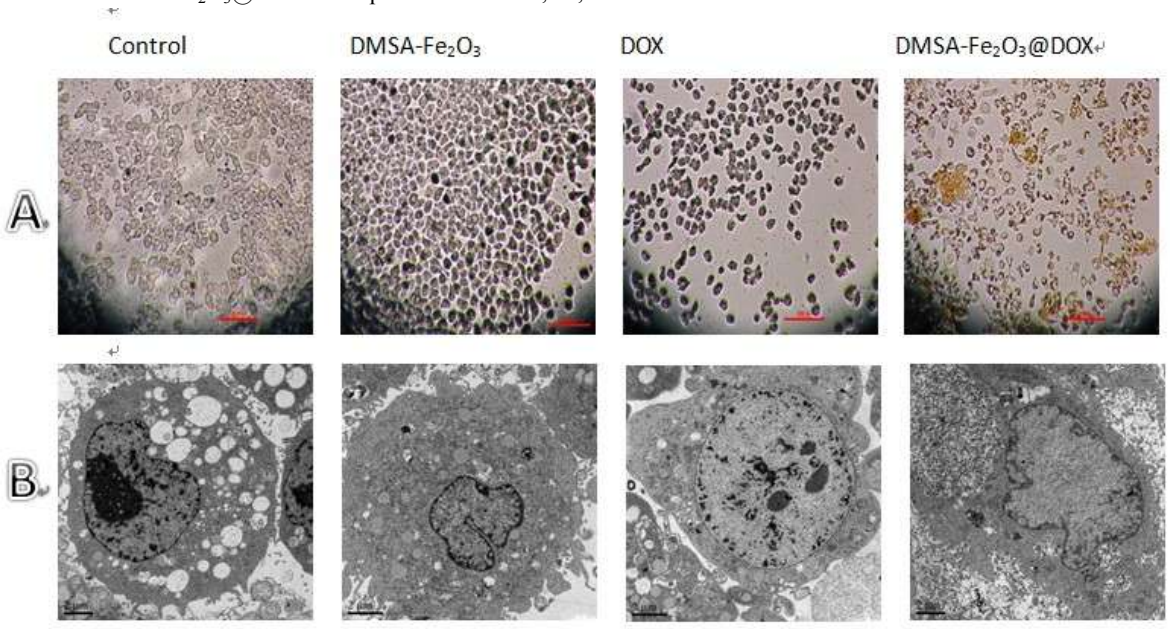

Figure 7. Morphological observation of HepG2 cells, untreated (control) and treated with DMSA-Fe_2O_3 magnetic nanoparticles, DOX and DMSA-Fe_2O_3 @DOX at a concentration of 9.0 µg/well and 24 h. A: Optical microscopic images of HepG2 cells. B: Transmission electron microscopic observation of HepG2 cells.

4. CONCLUSIONS

In summary, we successfully synthesized DMSA-Fe_2O_3@DOX via a simple and effective method. The DOX loading rate was as high as 87% after optimizing reaction conditions. Drug loading on superparamagnetic nanoparticles can be delivered to the desired site, which is of significance for cancer target therapy. It also indicated that DMSA-Fe_2O_3 did not show any significant cytotoxic activity in HepG2 cells, whereas it was

slightly more cytotoxic for HepG2 cells treated with DMSA-Fe_2O_3@DOX than those treated with DOX alone.

5. REFERENCES

[1]R. Siegel, D. Naishadham and A. Jemal, Cancer statistics, 2012, *CA: A Cancer Journal for clinicians*, 63, 11-30, **2013**.

[2] F. S. Carvalho, A. Burgeiro, R. Garcia, A. J. Moreno, R. A. Carvalho and P. J. Oliveira, Doxorubicin-induced cardiotoxicity: from bioenergetic failure and cell death to cardiomyopathy, *Medicinal Research Reviews*, 0, 1-30, **2013**.

[3] T. H. Kim, C. W. Mount, W. R. Gombotz, S. H. Pun, The delivery of doxorubicin to 3-D multicellular spheroids and tumors in a murine xenograft model using tumor-penetrating triblock polymeric micelles, *Biomaterials*, 31, 7386-7397, **2010**.

[4] A. M. Nowicka, A. Kowalczyk, A. Jarzebinska, M. Donten, P. Krysinski, Z. Stojek, E. Augustin and Z. Mazerska, Progress in targeting tumor cells by using drug-magnetic nanoparticles conjugate, *Biomacromolecules*, 14, 828-833, **2013**.

[5] Z. Sun, V. Yathindranath, M. Worden, J. A. Thliveris, S. Chu, F. E. Parkinson, T. Hegmann and D. W. Miller, Characterization of cellular uptake and toxicity of aminosilane-coated iron oxide nanoparticles with different charges in central nervous systemrelevant cell culture models, *Int J Nanomedicine*, 8, 961-970, **2013**.

[6] N. Schleich, P. Sibret, P. Danhier, B. Ucakar, S. Laurent, R. N. Muller, C. Jerome, B. Gallez, V. Preat and F. Danhier, Dual anticancer drug/superparamagnetic iron oxide-loaded PLGA-based nanoparticles for cancer therapy and magnetic resonance imaging, *Int J Pharm*, 447, 94-101, **2013**.

[7] C. H. Fan, C. Y. Ting, H. J. Lin, C. H. Wang, H. L. Liu, T. C. Yen and C. K. Yeh, SPIO-conjugated, doxorubicin-loaded microbubbles for concurrent MRI and focused-ultrasound enhanced brain-tumor drug delivery, *Biomaterials*, 34, 3706-3715, **2013**.

[8] S. B. Campbell, M. Patenaude and T. Hoare, Injectable superparamagnets: highly elastic and degradable poly(N-isopropylacrylamide)–superparamagnetic iron oxide nanoparticle (SPION) composite hydrogels, *Biomacromolecules*, 14, 644-653, **2013**.

[9] G. Y. Lee, W. P. Qian, L. Wang, Y. A. Wang, C. A. Staley, M. Satpathy, S. Nie, H. Mao and L. Yang, Theranostic nanoparticles with controlled release of gemcitabine for targeted therapy and MRI of pancreatic cancer, *ACS Nano*, 7, 2078-2089, **2013**.

[10] H. Salehizadeh, E. Hekma tian and M. S. a. K. Kennedy, Synthesis and characterization of core-shell Fe3O4-gold-chitosan nanostructure, *J Nanobiotechnology*, 10, 1-7, **2012**.

[11] S. Ahmad, U. Riaz, A. Kaushik and J. Alam, Soft template synthesis of super paramagnetic Fe3O4 nanoparticles a novel technique, *Journal of Inorganic and Organometallic Polymers and Materials*, 19, 355-360, **2009**.

[12] S. Zhang, X. Chen, C. Gu, Y. Zhang, J. Xu, Z. Bian, D. Yang and N. Gu, The effect of iron oxide magnetic nanoparticles on smooth muscle cells, *Nanoscale Research Letters*, 4, 70-77, **2008**.

[13] J. Bhattacharjee, Gunjan Verma and V. a. P. A. Hassan, Small angle neutron scattering study of doxorubicin–surfactant complexes encapsulated in block copolymer micelles, *Journal of Physics*, 71, 991-995, **2008**.

[14] F. Xiong, Z. Y. Zhu, C. Xiong, X. Q. Hua, X. H. Shan, Y. Zhang N. Gu, Preparation, characterization of 2-deoxy-D-glucose functionalized dimercaptosuccinic acid-coated maghemite nanoparticles for targeting tumor cells, *Pharmaceutical Research*, **29**, 1087-1097, **2012**.

[15] M. M. Yallapu, S. P. Foy, T. K. Jain, V. Labhasetwar, PEG-functionalized magnetic nanoparticles for drug delivery and magnetic resonance imaging applications, *Pharmaceutical Research*, 27, 2283-2295, **2010**.

[16] M. Auffan, L. Decome, J. Rose, T. Orsiere, M. D. Meo, V. Briois, C. Chaneac, Luca Olivi, J.L.Berge-Lefranc, A. Botta, Mark R. Wiesner, A. J.-Y. Bottero, *In vitro* interactions between DMSA-coated maghemite nanoparticles and human fibroblasts: a physicochemical and cyto-genotoxical study, *Environmental Science & Technology*, 40, 4367-4373, **2006**.

[17] N. K. Jain and S. K. Jain, Development and In Vitro Characterization of Galactosylated Low Molecular Weight Chitosan Nanoparticles Bearing Doxorubicin, *AAPS PharmSciTech*, 11, 686-697, **2010**.

[18] F. Zhang, H. Yang, X. Xie, L. Li, L. Zhang, J. Yu, H. Zhao and B. Liu, *Sensors and Actuators B: Chemical*, Controlled synthesis and gas-sensing properties of hollow sea urchin-like α-Fe2O3 nanostructures and α-Fe2O3 nanocubes, 141, 381-389, **2009**.

[19] M. W. Amjad, M. C. I. Mohd Amin and H. K. a. A. M. Butt, Doxorubicin-loaded cholic acid-polyethyleneimine micelles for targeted delivery of antitumor drugs: synthesis, characterization, and evaluation of their in vitro cytotoxicity, *Nanoscale Research Letters*, 6, 687, **2012**.

[20] V. E. Bosio, V. Machain, A. G. Lopez, I. O. De Berti, S. G. Marchetti, M. Mechetti and G. R. Castro, Binding and encapsulation of doxorubicin on smart pectin hydrogels for oral delivery, *Applied Biochemistry and Biotechnology*, 167, 1365-1376,**2012**.

6. ACKNOWLEDGEMENTS

This study received financial support from Shandong provincial science and technology development plan (2012GSF12107), Taishan Scholar Construction Project, and a Project of Shandong Province Higher Educational Science and Technology Program (No.J12LD06).